mathematics

MDPI

Article

Intelligent Classification and Diagnosis of Diabetes and Impaired Glucose Tolerance Using Deep Neural Networks

Alma Y. Alanis [1], Oscar D. Sanchez [1,*], Alonso Vaca-González [2] and Eduardo Rangel-Heras [1,*]

[1] University Center of Exact Sciences and Engineering, University of Guadalajara, Guadalajara 44430, Mexico; alma.alanis@academicos.udg.mx
[2] Institutional Safety, Health and Environment System (SISSMA), University of Guadalajara, Guadalajara 44430, Mexico; alonso.vaca@redudg.udg.mx
* Correspondence: didier.sanchez@academicos.udg.mx (O.D.S.); eduardo.rangel@academicos.udg.mx (E.R.-H.); Tel.: +52-133-3814-2350 (ext. 44410) (O.D.S.); +52-181-2178-8320 (ext. 44410) (E.R.-H.)

Abstract: Time series classification is a challenging and exciting problem in data mining. Some diseases are classified and diagnosed based on time series. Such is the case for diabetes mellitus, which can be analyzed based on data from the oral glucose tolerance test (OGTT). Prompt diagnosis of diabetes mellitus is essential for disease management. Diabetes mellitus does not appear suddenly; instead, the patient presents symptoms of impaired glucose tolerance that can also be diagnosed via glucose tolerance testing. This work presents a classification and diagnosis scheme for diseases, specifically diabetes mellitus and poor glucose tolerance, using deep neural networks based on time series data. In addition, data from virtual patients were obtained through the Dalla Man and UVA/Padova models; the validation was carried out with data from actual patients. The results show that deep neural networks have an accuracy of 96%. This indicates that DNNs is a helpful tool that can improve the diagnosis and classification of diseases in early detection.

Keywords: deep neural network; diabetes; classification

MSC: 68T01

check for updates

Citation: Alanis, A.Y.; Sanchez, O.D.; Vaca-González, A.; Rangel-Heras, E. Intelligent Classification and Diagnosis of Diabetes and Impaired Glucose Tolerance Using Deep Neural Networks. *Mathematics* **2023**, *11*, 4065. https://doi.org/10.3390/math11194065

Academic Editor: Lin Lin

Received: 4 September 2023
Revised: 19 September 2023
Accepted: 22 September 2023
Published: 25 September 2023

Copyright: © 2023 by the authors. Licensee MDPI, Basel, Switzerland. This article is an open access article distributed under the terms and conditions of the Creative Commons Attribution (CC BY) license (https://creativecommons.org/licenses/by/4.0/).

1. Introduction

Health is one of the most critical issues in society, since people's quality of life is explicitly based on it. Therefore, prompt detection and correct diagnosis of diseases are as relevant as treatment since the patient is likely to improve according to decisions made by their doctor based on more and better information [1]. Sometimes, it is necessary to diagnose a person using statistical and computational methods. Because medical decision-making data consists of many heterogeneous variables obtained from various sources, such as demographics, disease history, medications, allergies, biomarkers, medical photographs or genetic markers, and sensors, each of these variables offers a unique, slightly different view of the patient's condition. Researchers and clinicians face several challenges when analyzing such data, such as dimensionality, the number of samples increasing exponentially in the feature space, and statistical features [2]. These causes contribute to delays and inaccuracies in diagnosing the disease, meaning that patients cannot obtain adequate care.

New approaches have emerged outside the traditional approach [2], providing a new vision that helps us detect overlooked aspects. Based on Artificial Intelligence (AI) methods, systematic analysis of human diseases has been proposed. As described in Ref. [3], blood cancer is automatically detected through imaging using convolutional neural networks, heart disease detection is performed [4], Alzheimer's disease diagnosis is achieved with the help of a vector machine classifier [5], and using a machine learning method, the classification of diabetes is achieved based on a high-dimensional medical data set [6]. In work published in Ref. [7], machine-learning models were used to classify the state of

glucose metabolism of non-diabetic individuals through the OGTT. However, the results show low precision and do not consider patients with impaired glucose tolerance and diabetes mellitus.

On the other hand, deep neural networks (DNNs) have enabled significant advances in the fields of sound and image processing [8,9], sequential data [10], and solving detection problems using multivariate time series of vibration signals [11]. Moreover, DNNs have attracted the attention of researchers in medicine. For instance, the work [12] reported using deep learning to diagnose diseases such as Parkinson's, heart failure in Ref. [13] or losses in the sensors of medical equipment [10]. Several works have focused on using image analysis to detect different diabetes types and related illnesses. Big Sheng et al. overviewed the artificial intelligence applications in diabetic retinopathy and other ocular diseases. They reported several studies implementing the consultative neural network to detect ills by processing images and illnesses, such as diabetic retinopathy, cataracts, glaucoma, and age-related macular degeneration [14]. Akihiro Nomura et al. present a report in which machine learning (ML) models are used to predict diabetes mellitus (DM) in no-diabetes patients 5–10 years old. The models are random forest, logistic regression, and gradient boosting. The AUC increases from 0.71 to 0.87 [15]. Ivan Contreras and Josep Vehi present a review of several papers about blood glucose prediction. Some of the techniques used include k-means, fuzzy logic, heuristic methods, random forest, and support vector machines. The prediction horizon increases from 15 to 180 min. According to the review paper, some inputs to the algorithms include glucose absorption via carbohydrate consumption and insulin infusion [16]. Jyotismita Chaki et al. present a systematic review of machine learning and artificial intelligence for the analysis of DM detection, diagnosis, and self-management techniques. Some of the methods used include KNN, SVM, DT, GA, RF, CNN, FFNN, Region convolutional neural networks, MLP, and pattern recognition neural networks. The ML techniques focus on image classification (shape, color, and texture features) and text features like glucose level, age, heredity, and other factors [17]. For this work, the diagnosis and classification of diabetes mellitus through time series are proposed.

Diabetes mellitus (DM) is a metabolic disorder which is characterized by high glycemia and difficulty metabolizing carbohydrates [18,19]. Prolonged hyperglycemia due to diabetes is associated with microvascular and macrovascular complications that affect the kidneys, nerves, and eyes and lead to the risks of cardiovascular diseases [20]. It is classified into different types depending on its etiology and pathophysiological mechanisms. The most frequent is type 2, which consists of several factors, including carbohydrate intolerance and metabolic syndrome, which stems from insulin resistance [21,22].

The diagnostic criteria for diabetes are based on glycemic thresholds associated with microvascular disease. These criteria use blood samples, intravenous line, and laboratory analysis methods [20]; for instance, Fasting Plasma Glucose (FPG) level, 2-Hour Plasma Glucose (2hPG), 75 g Oral Glucose Tolerance Test (OGTT) and Hemoglobin A1c (HbA1c) test. However, one of the most objective, easy, and economical ways to identify the absorption and distribution of serum glucose in the body is by quantifying it postprandially with the help of the glucose tolerance curve test [18,23].

Many other associated biomarkers have been described. However, these markers have not been used as determinants for the development of DM on their own or in conjunction with other factors, since they have turned out to be non-specific for DM and only describe a state of chronic inflammation. In addition, establishing changes in the hormone-level disorders associated with metabolic syndrome is extremely difficult, uncomfortable, and expensive for patients.

In this work, we focus mainly on changes in the absorption and bioavailability of carbohydrates, which is the cornerstone of DM, as a starting point for changes in glucose intolerance, which is not considered to be a form of diabetes, but could be an indicator that the person will develop diabetes in the future. Therefore, serum glucose-independent biomarkers provide poor certainty and information for identifying and preventing the development of diabetes or prediabetes or their complications. Therefore, having the ability

to identify variations and trends from the glycemic curve alone and predict its behavior could be extremely beneficial for the diagnosis, monitoring, and treatment of people with carbohydrate disorders through time series.

Since the use of time series for classifying patients with diabetes mellitus and impaired glucose tolerance is proposed in this work, the information generated by the OGTT is used. Also, we suggest using neural networks for the rapid and accurate detection and diagnosis of human diseases based on serial time data of blood glucose sensors. These deep neural networks are the long-short-term memory (LSTM), multilayer neural network (MLP), convolutional neural network, LSTM-recurrent neural network (LSTM-RNN), LSTM-fully convolutional networks (LSTM-FCN) and residual neural network (ResNet). The main contributions are described as follows:

1. Serial data classification is performed using deep neural networks.
2. Data from healthy patients, as well as patients with impaired glucose tolerance and with diabetes mellitus were generated by means of Dalla Man and UVA/Padova mathematical models.
3. The classification performance of the proposed deep neural networks is compared.
4. The neural classifiers are validated with serial data from real patients.

2. Methodology

Deep neural networks must be trained on a large amount of data in order to work and to achieve good classification results. However, it is not always easy to obtain this information due to particular characteristics with which it must be obtained. An example of this is the glucose tolerance test, which must be performed under the supervision of a doctor, which takes time, availability and patient permissions. We propose that data be generated from mathematical models recognized in the literature regarding glucose dynamics; these data serve as input for training intelligent algorithms and validating them with real data. The objective of the work is to verify if deep neural networks are capable of detecting impaired glucose tolerance, a state in which one is not healthy but is not considered diabetic, which can be difficult to detect even for doctors. This study also corroborates the possibility of using data from virtual patients obtained from the glucose tolerance test in the training of intelligent algorithms and maintaining the classification and detection performance with real patients.

For this study, data were first generated from patients with diabetes mellitus, impaired glucose tolerance, as well as data from people with normal glucose ranges according to the Oral Glucose Tolerance Test. The virtual patients were carefully classified by a doctor according to the Oral Glucose Tolerance Test criteria (described later) into their respective classes (diabetes mellitus, impaired glucose tolerance and normal). The classified data serve to feed the artificial intelligence algorithms for training and testing. In the same way, using the Oral Glucose Tolerance Test, data from real patients are obtained for validation.

Figure 1 shows the flow diagram for the methodology; first, we generate the time series with the UVA/Padova Diabetes simulator, then the dataset is split up into two parts: 70% for training (training stage) and 30% for testing (testing stage). Once we have good agreement in the testing stage, we use the development models to classify the data (from real patients) into normal, impaired glucose tolerance and DM patients.

The paper is organized as follows. First, a review of the DNNs and machine learning techniques is included. Next, the Oral Glucose Tolerance Test is described. Then, the proposed scheme for simulated data acquisition is presented. Subsequently, the real data patients used for classification are shown. Later, the results are presented, and finally, the conclusions and future works are stated.

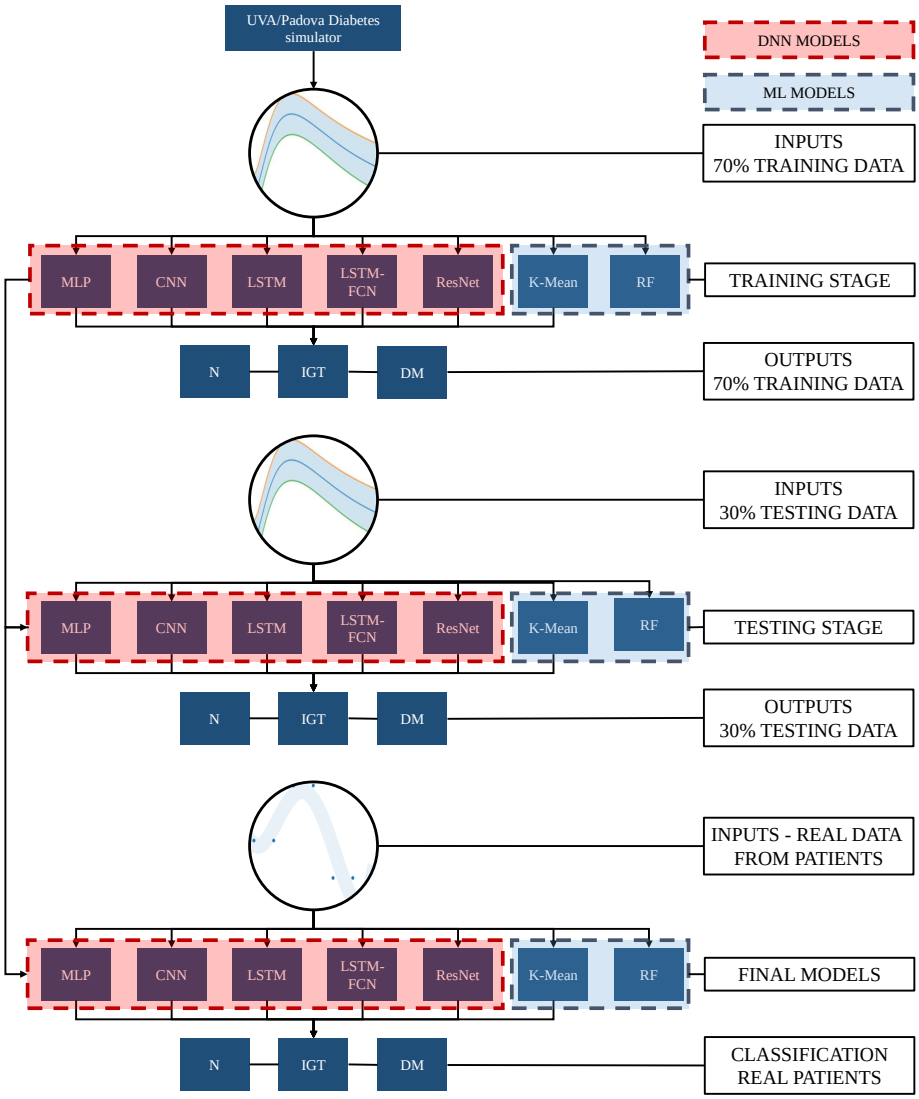


Figure 1. Flow diagram for methodology. Red box for DNN models and blue for ML models

3. Deep Neuronal Network for Time Series Classification

3.1. Time Series Classification

Time Series Classification is considered a challenging problem. Commonly, the data series in real applications comprise information acquired through sensors in real time. Time series illustrate a relationship between past and present data to confirm trends.

A time series is defined as a vector $X = [x_1, x_2, \ldots, x_n]$ composed of real values. The size of the vector corresponds to the number of samples n that it contains.

Thus, the dataset $D = \{(X_1, Y_1), (X_2, Y_2), \ldots, (X_N, Y_N)\}$ is a collection in which X_i is a time series and Y_i is its class label vector. The length of Y_i corresponds to the number of classes k, where each element $j \in [1, k]$ is equal to one if the class of X_i is j and zero otherwise.

Then, the dataset D is used to generate deep neural network models with the ability to create a probability distribution of the classes based on the space of possible inputs.

3.2. Deep Neural Networks

Neural networks with shallow architectures limit the learning of complex nonlinear relationships [24]. On the other hand, the so-called DNNs contain multiple layers of

nonlinear operations that allow them to capture complex dynamics by training the multiple layers [25].

Models generated by deep neural networks offer a promising approach to automatic feature extraction from complex data model representations [26]. Furthermore, through the data obtained via sensors, the DNNs can contribute to developing better and more reliable diagnosis and disease classification systems, improving upon the current diagnostic methods.

Therefore, DNNs are proposed in this work to classify and detect diabetes and impaired glucose tolerance from data observed using glucose sensors generated via the glucose tolerance test. The neural networks used are MLP, Convolutional Neural Network (CNN), LSTM, LSTM-FCN, and ResNet, all of which are described below.

3.3. Multilayer Perceptron Neural Networks

Among the neural network models, the multilayer perceptron (MLP) is one of the most popular and influential, and is used in various problems [27,28]. For example, due to its efficiency and flexibility, the MLP has been used in classification applications [28]. Generally, a multilayer neural network comprises an input layer, followed by one or more hidden layers, and a feed-forward output layer. Dense layers are composed of two or more hidden layers with several nodes connected to nodes of neighboring hidden layers by their weights.

The following equation describes the output of neuron j in the hidden layer.

$$s_j = \sigma\left(\sum_{i=1}^{n} w_{ji}x_i + b_i\right) \tag{1}$$

where w_{ji} are weights and b_i are biases of the hidden layer, and σ is the sigmoid activation function.

Then, the output of an MLP network y is calculated according to the following equation:

$$y = \sigma\left(\sum_{j=1}^{m} w_{kj}s_i + b_0\right) \tag{2}$$

where w_{kj} are weights and b_0 are biases of the hidden layer, and σ is the sigmoid activation function.

3.4. Convolutional Neural Network

Convolutional neural network (CNN) has been primarily applied in object recognition, image classification, and recently in time series classification [29–31].

CNN has been generally used for information that can be represented in 2D arrays. On the other hand, 1-D architectures have been used in the convolution layer. In this architecture, 1-D cores are operated, and 1-D filters are used on the input signal. However, there are few works that relate to the classification and detection of disease using the 1-D convolutional neural network.

The filter bank layer is composed of filters applied over the input layer. The output of this layer corresponds to the convolution of the weights of the neurons with the input. The result is a new feature map set [32].

The nonlinear function Rectified Linear Unit (ReLU) is used in the nonlinearity layer of the convolutional neural network to trim the output; the mathematical function is presented below:

$$ReLU = \begin{cases} 0, & if \quad x < 0, \\ x, & if \quad x \geq 0. \end{cases} \tag{3}$$

The feature pooling layer is used to reduce the dimension of the inputs. The commonly used methods in this layer are max pooling and mean pooling.

Finally, in the output layer, the softmax layer is used to increase the maximum probability of the output. The softmax function is presented below

$$o_i = \frac{e^{z_i}}{\sum_{i=1}^{N} e^{z_i}}, \tag{4}$$

where o represents the network's output after the softmax layer, z is the neural network's output before the softmax layer, and N represents the number of classes or outputs.

3.5. Long Short-Term Memory Recurrent Neural Network

The LSTM recurrent neural network proposed in Ref. [33] solves the vanishing gradient problem presented by recurrent neural networks. Furthermore, LSTM introduces a forget gate to control the memory of past states; in general, the LSTM is described by the following equations [34]:

$$i_t = \sigma(W_{x_i} x_t + W_{h_i} h_{t-1} + W_{c_i} c_{t-1} + bi) \tag{5}$$

$$f_t = \sigma(W_{x_f} x_t + W_{h_f} h_{t-1} + W_{c_f} c_{t-1} + bf) \tag{6}$$

$$\widetilde{C}_t = tanh(W_{x_c} x_t + W_{h_c} h_{t-1} + bc) \tag{7}$$

$$C_t = f_t C_{t-1} + i_t \widetilde{C}_t \tag{8}$$

$$o_t = \sigma(W_{x_o} x_t + W_{h_o} h_{t-1} + W_{c_o} C_t + bo) \tag{9}$$

$$h_t = o_t tanh(C_t) \tag{10}$$

where Ws are weight matrices and bs are biases. f, i, o are the forget, input, and output gates, respectively. σ is the sigmoid logistic function, C is the so-called cell activation, and ht is the value between -1 and 1 of the output gate value scaled by the $tanh$ function.

3.6. LSTM Fully Convolutional Networks

LSTM-FCN is a deep learning method proposed in Ref. [35] for the classification of time series data. LSTM-FCN is made up of two blocks: a convolutional block and an LSTM block that receives the same time series as input, as shown in Figure 2.

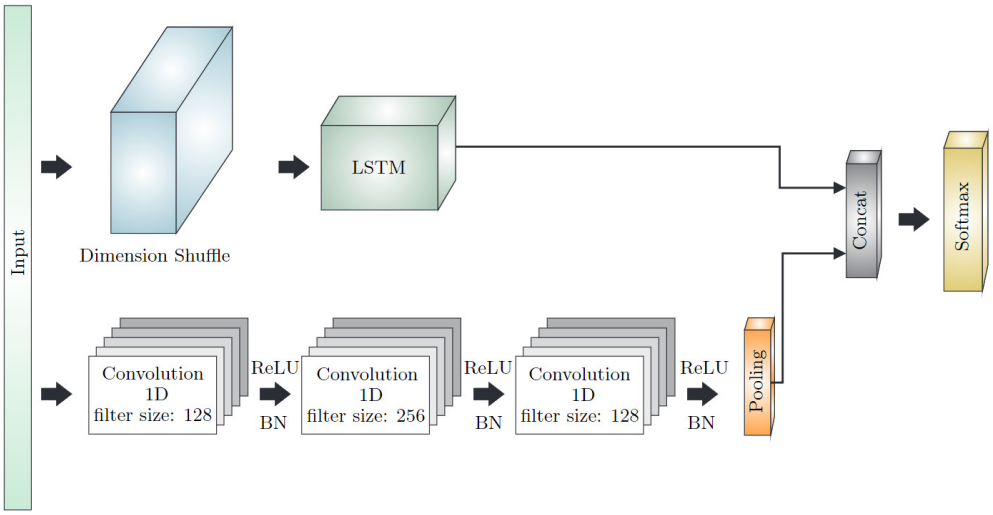


Figure 2. LSTM-FCN architecture.

The convolutional block contains convolutional layers with filters of 128, 256, and 128, respectively. The architecture proposed in Ref. [36] is followed by the ReLU activation function. Features are then extracted using global average pooling.

Simultaneously, the time series input is dimensioned and passed through the LSTM block. Next, the output of the LSTM and the output of the feature extraction layer are concatenated. Then, the multiclass classification is generated through a softmax layer [37].

3.7. Residual Deep Networks

Residual networks (ResNet) is a deep neural network presented in Ref. [38], which is composed of stacked "Residual Units". ResNets can be represented in their general form as:

$$y_l = x_l + F(x_l) \tag{11}$$
$$x_{l+1} = \theta(y_l),$$

where x_l is the input, $x_l + 1$ is the output of unit l, $\mathcal{F}$ represents the residual function. θ is the ReLU activation function [38]. $F(x_l) + x_l$ is achieved by feedforward neural networks with "shortcut connections" (Figure 3).

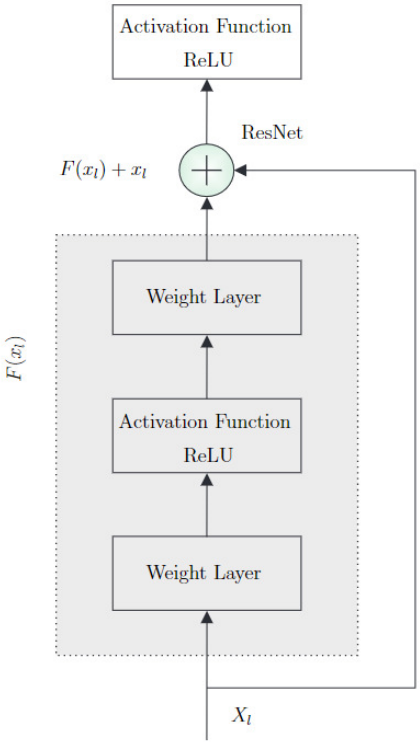


Figure 3. Building block of a ResNet.

ResNets are made up of more than 100 deep layers and have shown remarkable accuracy in complex reconnaissance tasks [39,40].

The main idea of ResNets is to learn the additive residual function F relative to x_l. This is achieved by attaching a shortcut or jump connection to move between multiple layers. They accomplish this by using shortcuts or "jump connections" to move over various layers.

4. Machine Learning Models

Deep neural networks are compared with two popular machine learning techniques commonly applied in classification: K-means and Random Forest.

4.1. Random Forest

Random forest (RF) is a common and efficient algorithm among machine learning techniques for data classification. RF produces forests with decision trees (DT), and enough trees can improve predictions. Characteristics are essential to defining new models; each

tree provides an identification ballot, and the tree label maintains the model. The forest chooses the party with the highest ballot numbers. That is, the classification process of the RF is closely related to the strategy of the baggage. RF generates a training subgroup and builds a DT for each subset. Once all DTs have determined every input vector for the collection of tests, the forest finally chooses the one with the most ballots [17].

4.2. K-Means

K-means is a popular method of grouping. This method is iterative, numerical, non-deterministic, and unsupervised. K-means has been successfully applied to the classification research as described in Refs. [41,42].

In K-means, groups are generated, and the mean value of the elements in the group represents each group. A set of n elements is partitioned in k classes so that the similarity between clusters is low and the similarity between elements within the cluster is high. The Euclidean distance measures the resemblance.

In general, the K-means algorithm divides the elements into K categories $C = \{c_1, c_2, \ldots, c_k\}$. Each C has a clustering center μ_k. Then, the Euclidean distance equation is used to calculate the sum of the squares of the distances between the elements x_i of the class and the center of the cluster μ_k:

K-means minimizes the mean of the squared sum of the distance:

$$mean(c_k) = \sum_{x_i \in c_k} x_i - \mu_k \tag{12}$$

$$mean(K_c) = \sum_{k=1}^{K} mean(c_k) \tag{13}$$

5. Oral Glucose Tolerance Test

The OGTT consists of a patient taking a standardized glucose load and subsequent monitoring of serum glycemia in short periods, usually at 30 or 60 min until the 2 h mark is reached. This technique has been modified over the years [43]. It is established that this test must be performed in the morning with at least three days of a free diet; that is, (>150 g CHO), accompanied by physical activity. The patient should fast for at least 10 h but less than 16 h; they are permitted to drink water. The patient must remain seated, and smoking is prohibited throughout the test. A fasting blood sample is collected, and at time zero, the glucose dose of 75 g (1.75 g/kg ideal body weight) is ingested in a concentration not exceeding 25 g/dL of flavored water. Blood samples are collected at 30 min intervals for two h [21,23,44].

Conventionally, this test can classify patients in three stages: diabetic patients, patients with glucose intolerance or prediabetes, and healthy patients according to the current criteria of the ADA, with the advantage of greater sensitivity when analyzing more than a single measurement, in addition to baseline [18]. Table 1 shows the diagnostic criteria.

Prediabetes or glucose intolerance is the conventional term used to identify people whose glucose levels do not meet the criteria for diabetes but have an abnormal carbohydrate metabolism, with their numbers trending upwards. This indicates a high probability of developing diabetes in the near future [18,21,23,45].

Some of the advantages offered by OGTT are:

- OGTT recognizes altered postprandial metabolism, making it a method capable of detecting diabetes more efficiently than plasma glucose concentration and overnight fasting (FPG).
- An altered fasting blood glucose (IFG) has a normal 2hPG established by OGTT.
- FPG does not provide relevant metabolic information.

However, variations in the glycemic curve and sporadic low intakes cause the study's sensitivity to decrease. As a result, biases appear in the diagnosis, in addition to the fact

that there is no standardized predictive method of complications of the disease according to this method [18,21,23,45].

Table 1. OGTT Diagnostic criteria.

Diabetes Mellitus in Nonpregnant Adult		
Fasting value:	$\frac{1}{2}$-h, 1-h, or 1 $\frac{1}{2}$-h OGTT:	2-h OGTT:
venous plasma $\geq$ 140 mg/dL (7.8 mmol/L) venous whole blood $\geq$ 120 mg/dL (6.7 mmol/L) capillary whole blood $\geq$ 120 mg/dL (6.7 mmol/L)		venous plasma $\geq$ 200 mg/dL (11.1 mmol/L) venous whole blood $\geq$ 180 mg/dL (10.0 mmol/L) capillary whole blood $\geq$ 120 mg/dL (6.7 mmol/L)
Impaired Glucose Tolerance (IGT) in Nonpregnant Adults		
Fasting value:	$\frac{1}{2}$ h, 1 h, or 1 $\frac{1}{2}$ h OGTT:	2 h OGTT:
venous plasma $<$ 140 mg/dL (7.8 mmol/L)	venous plasma $\geq$ 200 mg/dL (11.1 mmol/L)	venous plasma of between 140 and 200 mg/dL (7.8 and 11.1 mmol/L)
venous whole blood $<$ 120 mg/dL (6.7 mmol/L)	venous whole blood $\geq$ 180 mg/dL (10.0 mmol/L)	venous whole blood of between 120 and 180 mg/dL (6.7 and 10.0 mmol/L)
capillary whole blood $<$ 120 mg/dL (6.7 mmol/L)	capillary whole blood $\geq$ 200 mg/dL (11.1 mmol/L)	capillary whole blood of between 140 and 200 mg/dL) (7.8 and 11.1 mmol/L)
Normal Glucose Levels in Nonpregnant Adults		
Fasting value:	$\frac{1}{2}$ h, 1 h, or 1 $\frac{1}{2}$-h OGTT:	2 h OGTT:
venous plasma $<$ 115 mg/dL (6.4 mmol/L) venous whole blood $<$ 100 mg/dL (5.6 mmol/L) capillary whole blood $<$ 100 mg/dL (100 mmol/L)	venous plasma $<$ 200 mg/dL (11.1 mmol/L) venous whole blood $<$ 180 mg/dL (10.0 mmol/L) capillary whole blood $<$ 200 mg/dL (11.1 mmol/L)	venous plasma $<$ 140 mg/dL (7.8 mmol/L) venous whole blood $<$ 120 mg/dL (6.7 mmol/L) capillary whole blood $<$ 140 mg/dL (7.8 mmol/L)

To this end, other laboratory techniques have been developed to facilitate diagnosis, such as the fraction 1c of the glycated hemoglobin (HbA1c), which gives the estimate of the average glycemic figures during approximately the last three months, which is an excellent advantage in the diagnosis of the disease with already established patterns. However, it provides little certainty and information to identify and prevent the development of diabetes or prediabetes, as well as the prevention of diabetes complications [19,21,23,46]. To achieve this, it is necessary to identify changes in metabolic dysfunction from the beginning of its formation. One such change could be insulin resistance, a condition linked to metabolic syndrome; the first is a biochemical–molecular concept, where insulin has a lower biological efficiency when internalizing in cells due to multiple causes involving the same hormone or the behavior of its specific receptor or receptors. Meanwhile, the metabolic syndrome is a clinical concept characterized by the association of several diseases linked pathophysiologically through insulin resistance and hyperinsulinemia [18]. Being able to establish changes in the disorders of the levels of these hormones is extremely difficult and uncomfortable, and expensive for patients; therefore, having the ability to identify the variations and trends only with the glycemic curve to the stage and predict their behavior will help the attending physician to address health problems promptly before their complications occur or before the disease itself appears, with the lowest number of blood glucose intakes. In addition, the proposed models could benefit the hospital and home systems, implementing them in real-time quantification devices such as Abbott's LifeStyle (trademark) or even sophisticated software in hospitals and diagnostic laboratories.

6. Simulated Data Acquisition

Deep neural networks need to learn a large amount of data and information for their hidden layers. However, it is not easy to obtain so much sensitive information on patients with diabetes mellitus.

On the other hand, models have been developed to simulate the glucose–insulin system, helping us to study DM. They have also been used to design, test, and validate control algorithms designed to create an "artificial pancreas".

These models are widely accepted for preclinical tests, since different experimental scenarios can be investigated, reducing costs and time. As a result, the models of Dalla man and Uva/Padova are used to obtain oral glucose tolerance test data.

The Dalla Man model presented in Ref. [47] is a compartmental model. It is based on differential equations representing organs and tissues to describe the physiological events that occur after a meal. This model simulates the glucose–insulin system of a normal human being.

For its part, the UVA/Padova Diabetes simulator is representative of a DM population observed in a clinical trial [48]. Also, this T1DM Simulator has been accepted by the Food and Drug Administration (FDA) as a substitute for preclinical trials of specific insulin treatments such as closed-loop algorithms [49].

Based on these two models, different glucose tolerance tests were performed with varying scenarios of diabetes and healthy patients, modifying the most sensitive parameters published in work [50]. These include V_g,V_I,k_{p2}, k_1,k_2, k_{p1}, k_i, k_{e1}, k_{max}, k_{min}, k_{abs}, k_{p3}, k_{gri}. Each of the curves was carefully classified by a doctor according to the criteria published in work [51], previously described. A total of 441 healthy patients, 865 patients with impaired glucose tolerance, and 668 with diabetes were obtained.

Figures 4–6 show the average of the data obtained and the standard deviation for healthy patients, impaired glucose tolerance, and those with diabetes, respectively.

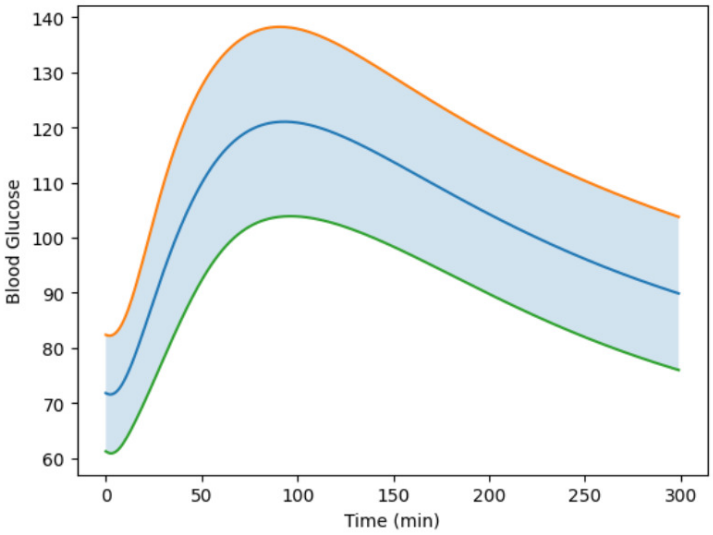


Figure 4. The average blood glucose (blue line) of the patients diagnosed as healthy obtained via the Dalla Man model ± the standard deviation (orange and green lines, respectively).

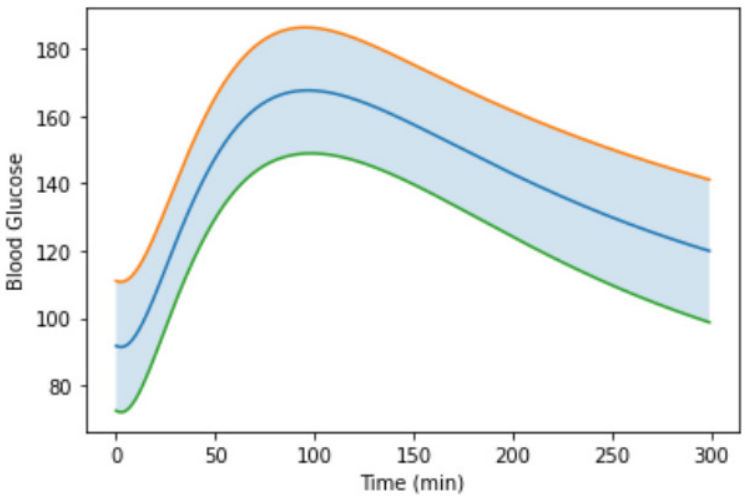


Figure 5. The average blood glucose (blue line) of the patients diagnosed with impaired glucose tolerance obtained via the UVA/Padova model ± the standard deviation (orange and green lines, respectively).

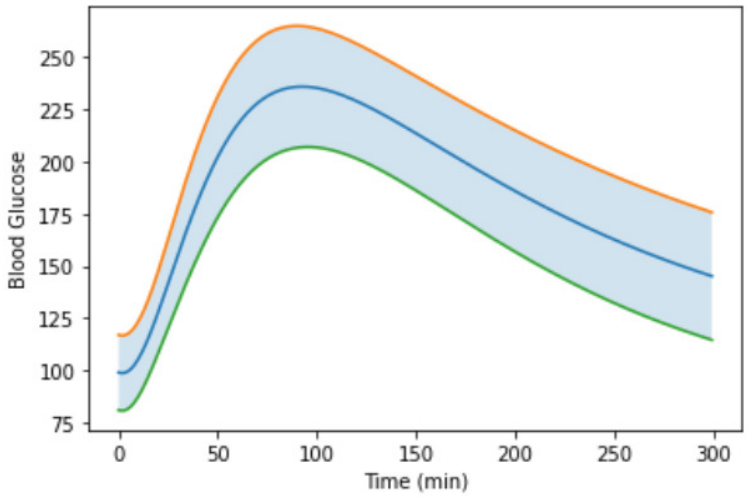


Figure 6. The average blood glucose (blue line) of patients diagnosed with diabetes obtained via the UVA/Padova model ± the standard deviation (orange and green line, respectively).

7. Real Data Description

To validate the efficacy of the models for the classification and diagnosis of diabetes mellitus and impaired glucose tolerance, curves generated based on the glucose tolerance test of real patients were used. None of this information was provided when training the models. Figure A1 show tolerance tests to oral intake of real patients. Three of them were obtained in work [52]; and the rest were obtained under medical supervision.

The data consist of a population of 16 individuals under an open, observational, descriptive, cross-sectional, retrospective study. These are people who came to the clinic due to carbohydrate absorption disorders, with or without a definite diagnosis of diabetes mellitus. The selection criteria were people diagnosed with type I and II Diabetes Mellitus, people with insulin resistance syndrome, people with glucose intolerance, and men or women over 18 years of age and without serious complications due to DM. The exclusion criteria were people with gestational diabetes, Maturity Onset Diabetes of the Young (MODY), etc., incomplete or inconclusive laboratory tests, and withdrawal of consent to participate. The non-inclusion criteria were a lack of laboratory studies, fluctuations in treatment, undergoing steroid treatment, having a diagnosis of hyperthyroidism, or having a serious infection. The data were obtained through the glucose tolerance test, of which samples were obtained every 30 min. The data did not undergo previous treatment of any kind.

The diagnosis of the real patients is shown in Table 2.

Table 2. A medical diagnosis of real patients. N indicates the category of normal patient, IGT indicates impaired glucose tolerance, and DM represents a diabetic patient.

Patient	a)	b)	c)	d)	e)	f)	g)	h)	i)	j)	k)	l)	m)	n)	o)	p)
Diagnosis	N	IGT	N	DM	N	N	N	IGT	IGT	N	N	IGT	N	N	IGT	IGT

8. Results

This section shows the results obtained with the neuronal classifiers for the diagnosis and classification of patients with diabetes, patients with impaired glucose tolerance, or healthy patients. One of the most widely used criteria for evaluating the classification capacity between different methods is the Receiver Operating Characteristic (ROC) curve.

This criterion generally compares the TP true-positive and FP false-positive rates that vary between other cut-off points. When $TP = FP$, a line is generated on the ROC curve showing random or poor classification performance. Therefore, the higher the line on the ROC curve, the better classification performance the method shows. If the process

can separate all TP cases from FP cases, the curve passes through the points $TP = 1$ and $FP = 0$ [53].

A summary of this criterion is the area under the curve (AUC). The higher the AUC, the better the ability of a classification method to distinguish between classes.

On the other hand, the confusion matrix shows a detailed summary of the results obtained using the classification models.

TP (classification correctly identified as positive cases) and TN (cases correctly classified as a negative class) are considered. FN (cases incorrectly classified as a negative class) and FP (cases incorrectly classified as a positive class) are also considered. This information obtained from the confusion matrix is used to evaluate the neural models with the following criteria.

Classification accuracy (CA) indicates the relationship between the number of correct predictions concerning the total number of samples.

$$CA = \frac{TP + FP}{TP + TN + FP + FN} \tag{14}$$

Precision (P) shows the classification performance of the DNNs of the true positives with respect to the false positives.

$$P = \frac{TP}{TP + FP} \tag{15}$$

The *Recall* (R) provides information on the number of true positives correctly identified.

$$R = \frac{TP}{TP + FN} \tag{16}$$

Finally, the score of $F1$ is helpful when the distribution of classes is uneven. This metric is obtained by combining P and R to compare the combined performance of *Precision* and *Recall* between various solutions.

$$F1 = 2 * \frac{P * R}{P + R} \tag{17}$$

To avoid overfitting, the neural networks used 70% of the data for training and 30% for testing. The model avoids the overfit if the errors between training and testing data do not differ much. Finally, the models were tested with unknown data (data not used in the training or testing stages). The efficiency obtained based on the evaluation criteria for the different models is shown in Table 3, where the best results are in bold.

It should be noted that these networks were designed mainly to deal with images, but in this work, they are used for time series. Thus, some DNNs show better results than others, as in the convolutional neural network, which offers an CA around 0.96, R of 0.97, and $F1$ score of 0.96, which is mainly superior to the other DNNs. It can be seen that the k-means machine learning model shows promising results, but lower than those offered by the networks. The classification results of the real patient data are shown in Table 4. It can be seen that most models perform well, correctly classifying all patients, which motivates us to continue working on diagnosing diseases based on time series.

The results of the evaluation criteria on real subjects are presented in Table 5, again the best results are reported in bold.

The performance results of the ROC curves of the different deep neural classifiers are shown in Figures A2–A8 in Appendix A. According to the ROC curve, the best models are LSTM-FCN, LSTM, and CNN, with a macro-average curve of 1, 0.97, and 0.97, respectively, followed by MLP and K-means with a macro-average curve of 0.96 and 0.94, respectively. Finally, the worst model according to ROC curve is the ResNet model, with a macro-average curve of 0.89. See Figures A2–A8 in Appendix A.

Table 3. Performance results of the different models under the evaluation criteria described above.

Model	Class	AUC	CA	P(%)	R(%)	F1-Score
MLP	Normal	**0.99**	0.96121	0.99218	0.94074	0.96577
	IGT	**0.99**	0.96121	0.96323	0.95272	0.95795
	Diabetes Mellitus	**1**	0.96121	0.93782	0.98907	0.96276
CNN	Normal	0.97	0.96795	0.97777	**0.97777**	0.97777
	IGT	0.97	0.96795	0.94755	**0.98545**	0.96613
	Diabetes Mellitus	0.97	0.96795	**0.99418**	0.93442	0.96338
LSTM	Normal	0.96	0.96290	0.94029	0.93333	0.93680
	IGT	0.96	0.96290	0.96691	0.95636	0.96160
	Diabetes Mellitus	0.99	0.96290	0.97326	**0.99453**	**0.98378**
LSTM-FCN	Normal	**0.99**	0.95784	**1**	0.92592	0.96153
	IGT	**0.99**	0.95784	0.94014	0.97090	0.95527
	Diabetes	**1**	0.95784	0.95652	0.96174	0.95912
ResNet	Normal	**0.99**	0.93591	0.99206	0.92592	0.95785
	IGT	0.94	0.93591	0.94382	0.91636	0.92988
	Diabetes Mellitus	0.94	0.93591	0.89	0.97267	0.92950
K-Means	Normal	0.93	0.925	0.88095	0.90243	0.89156
	IGT	0.93	0.925	0.93548	0.90625	0.92063
	Diabetes Mellitus	0.96	0.925	0.93846	0.96825	0.95312
RF	Normal	1	**0.97**	1	0.97560	**0.98765**
	IGT	0.97	**0.97**	**0.96875**	0.96875	**0.96875**
	Diabetes Mellitus	0.97	**0.97**	0.95312	0.96825	0.96062

Table 4. Classification results of real patients according to the different models. N indicates the category of average patient, IGT indicates impaired glucose tolerance, and DM represents a diabetic patient.

Model	MLP	CNN	LSTM	LSTM-FCN	ResNet	K-Means	RF
Patient	Diagnosis						
a)	N	N	N	N	N	N	N
b)	N	IGT	IGT	IGT	IGT	IGT	IGT
c)	N	N	N	N	N	N	N
d)	DM	DM	DM	DM	DM	DM	DM
e)	IGT	N	N	DM	N	N	N
f)	IGT	IGT	N	DM	N	IGT	N
g)	N	N	N	N	N	N	N
h)	IGT	IGT	IGT	DM	IGT	IGT	IGT
i)	N	DM	IGT	DM	DM	IGT	N
j)	N	N	N	N	N	N	N
k)	N	N	N	N	N	N	N
l)	N	IGT	IGT	DM	IGT	IGT	IGT
m)	N	N	N	N	N	N	N
n)	N	N	N	N	N	N	N
o)	N	IGT	N	DM	IGT	N	IGT
p)	IGT	IGT	IGT	IGT	IGT	IGT	IGT

Table 5. Performance results of the different models for real patients.

Model	Class	CA	P(%)	R(%)	F1-Score
MLP	Normal	0.82967	0.75280	0.99259	0.7
	IGT	0.82967	0.80208	0.84	0.4
	Diabetes Mellitus	0.82967	1	0.69398	1
CNN	Normal	0.96458	0.96376	0.98518	0.94117
	IGT	0.96458	0.94405	0.98181	0.83333
	Diabetes Mellitus	0.96458	1	0.92349	0.66666
LSTM	Normal	0.96121	0.94696	0.92592	**0.94736**
	IGT	0.96121	0.95985	0.95636	**0.90909**
	Diabetes Mellitus	0.96121	0.97326	0.99453	**1**
LSTM-FCN	Normal	0.96121	0.99230	0.95555	0.875
	IGT	0.96121	0.94366	0.97454	0.5
	Diabetes Mellitus	0.96121	0.96648	0.94535	0.25
ResNet	Normal	0.82967	0.85517	0.91851	1
	IGT	0.82967	0.95360	0.67272	0.90909
	Diabetes Mellitus	0.82967	0.72047	1	0.66666
K-Means	Normal	0.875	0.8888	0.8888	0.8888
	IGT	0.875	0.8333	0.8333	0.8333
	Diabetes Mellitus	0.875	1	1	1
RF	Normal	0.9375	1	0.9360	0.9
	IGT	0.9375	0.8333	0.9473	0.8
	Diabetes Mellitus	0.9375	1	1	1

9. Conclusions

Time series classification is challenging, but its medical applications are vast. There is a need to classify types and diagnoses of diseases from sensor-generated data accurately, rapidly, and cheaply. Deep neural networks are a reliable alternative for this task. In this work, models of deep neural networks for the classification and detection of diabetes mellitus and impaired glucose tolerance, in addition to differentiating from healthy patients using time serial data, were presented.

Due to the lack of information from patients with diabetes mellitus, impaired glucose tolerance, and healthy patients for the training of deep neural networks, the Dalla Man and Uva/Padova models were implemented to generate the glucose tolerance test to obtain serial data through the variation of more sensitive parameters of these models. From these models, 441 healthy patients, 865 patients with impaired glucose tolerance, and 668 with diabetes were obtained, and these were used for training and testing. The models were validated using serial data from patients who underwent glucose tolerance testing.

The results show superior performance to the traditional unsupervised machine learning method as K-means. The results presented by the random forest model in the virtual data are good, but in the real data, the random forest model shows an accuracy of around 93 % and an F1 score between 0.8 and 1; however, the LSTM shows slightly better results, with an accuracy of 96% and an F1 score between 9 and 1 on the real data, so the LSTM model is better at generalizing than random forest.

Furthermore, the results show that deep neural networks are a valuable tool for disease classification and diagnosis, showing an accuracy of around 96 % in most models. The LSTM neural network showed the best CA, R and $F1$ score criteria results in real data. The

rest of the networks presented a similar performance. However, the LSTM offers a higher AUC than the rest of the networks.

More real patients will be recruited for complete validation in future work.

Author Contributions: Conceptualization, A.Y.A. and O.D.S.; methodology, O.D.S.; software, O.D.S., A.Y.A. and E.R.-H.; validation, A.V.-G., O.D.S. and A.Y.A.; formal analysis, A.V.-G.; investigation, A.V.-G.; resources, A.Y.A. and O.D.S.; data curation, E.R.-H.; writing—original draft preparation, O.D.S., A.Y.A. and E.R.-H.; writing—review and editing, O.D.S., A.Y.A. and E.R.-H.; visualization, A.V.-G.; supervision, A.Y.A.; project administration, A.Y.A.; funding acquisition, A.Y.A. and O.D.S. All authors have read and agreed to the published version of the manuscript.

Funding: This research received external funding from CONACYT FOPI6-2021-01 number 319608.

Data Availability Statement: Data are available from the authors upon reasonable request.

Acknowledgments: The authors thank the University of Guadalajara for giving us the support to develop this research. We also thank conacyt for the financing provided for the project.

Conflicts of Interest: The authors declare no conflict of interest.

Appendix A

Appendix A.1. Real Patients Data

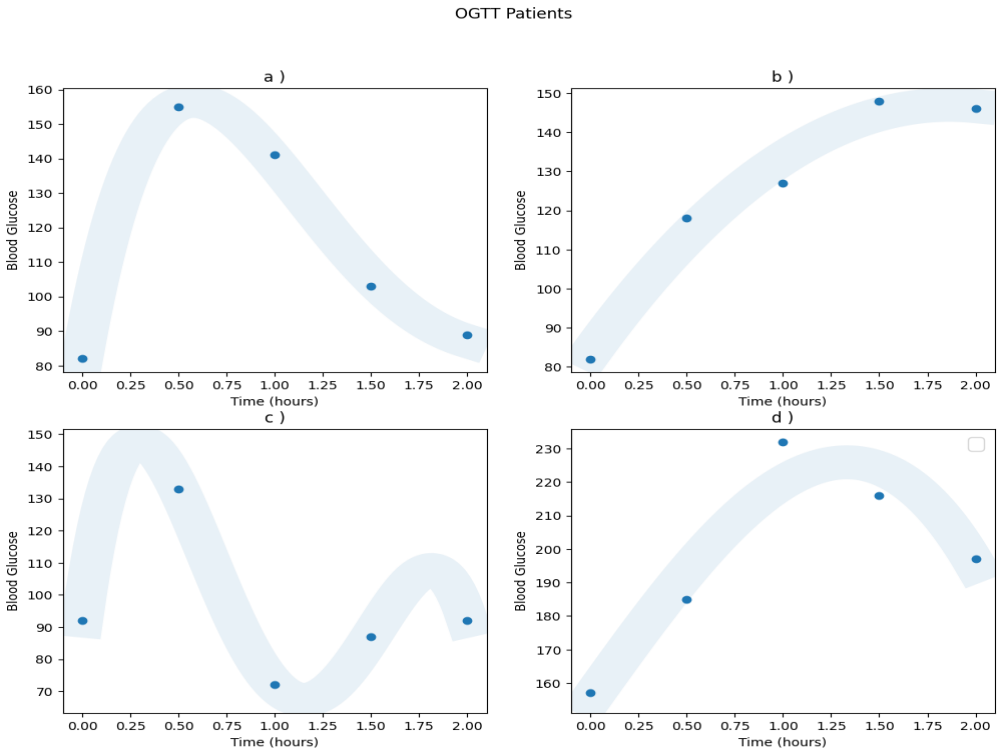


Figure A1. *Cont.*

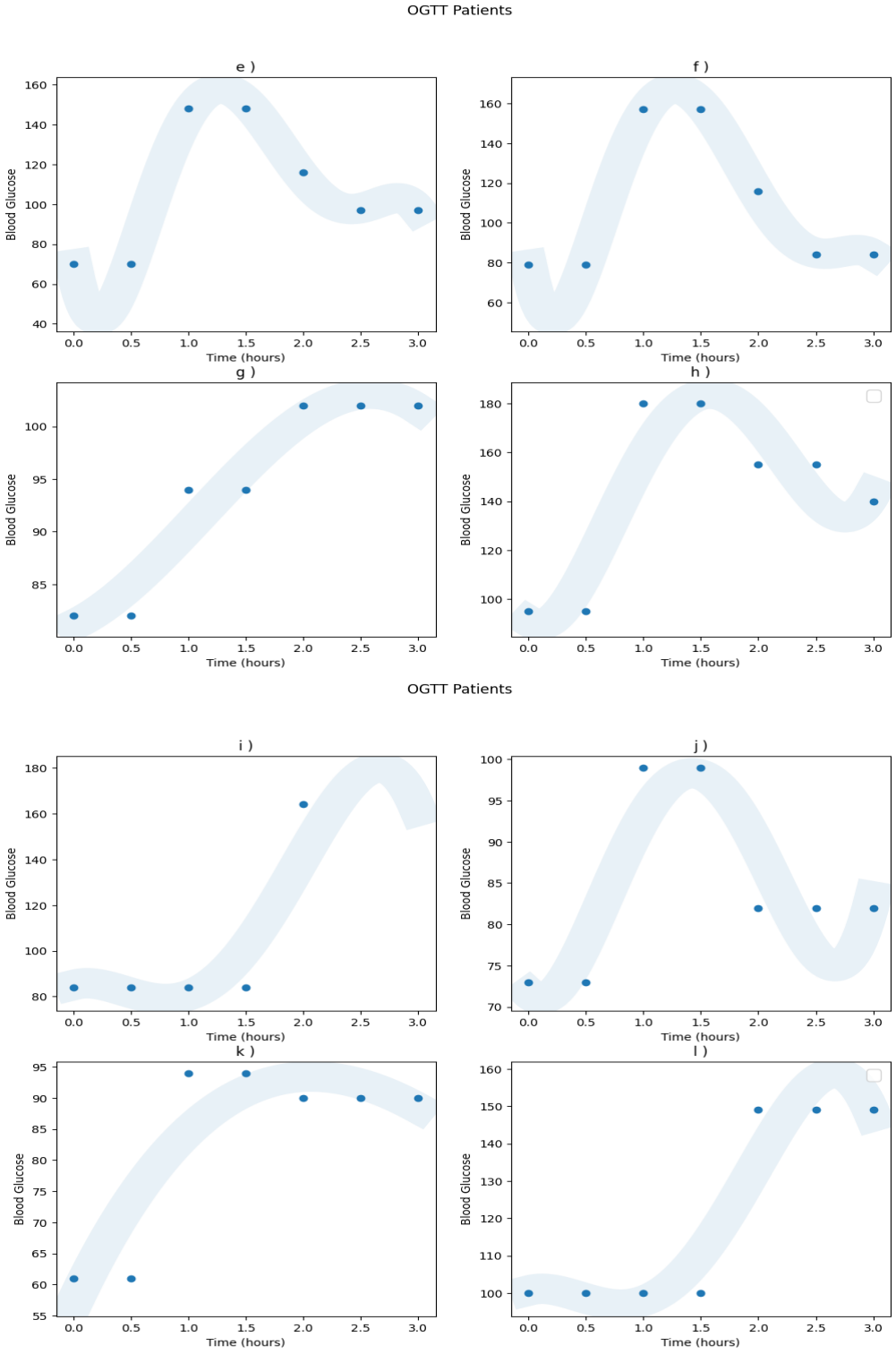


Figure A1. *Cont.*



Figure A1. Data obtained from the glucose tolerance tests of real patients. Where a)–p) represent real patients.

Appendix A.2. Models ROC Curves

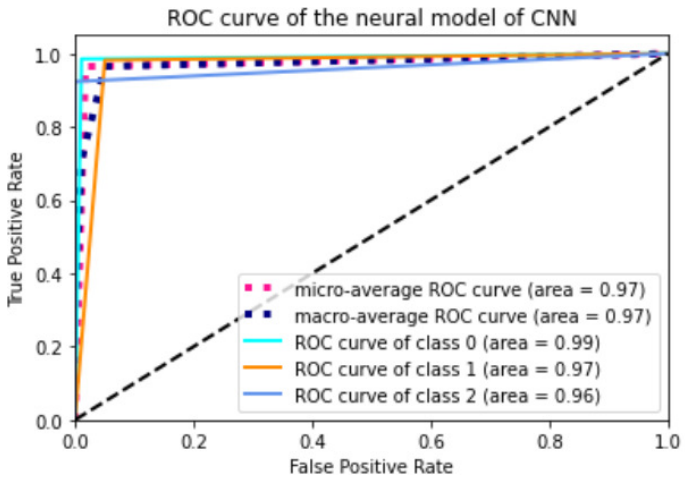


Figure A2. Classification performance of the CNN neural classifier. Class 0: normal patient, class 1: patient with glucose intolerance, and class 2: patient with diabetes mellitus.

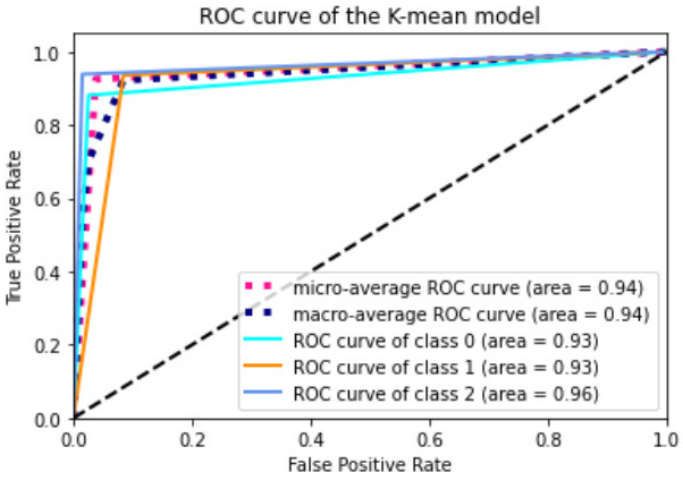


Figure A3. Classification performance of the K-means neural classifier. Class 0: normal patient, class 1: patient with glucose intolerance, and class 2: patient with diabetes mellitus.

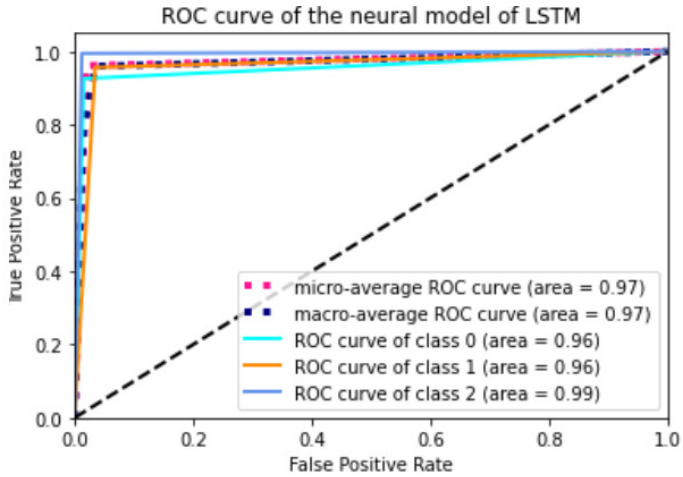


Figure A4. Classification performance of the LSTM neural classifier. Class 0: normal patient, class 1: patient with glucose intolerance, and class 2: patient with diabetes mellitus.

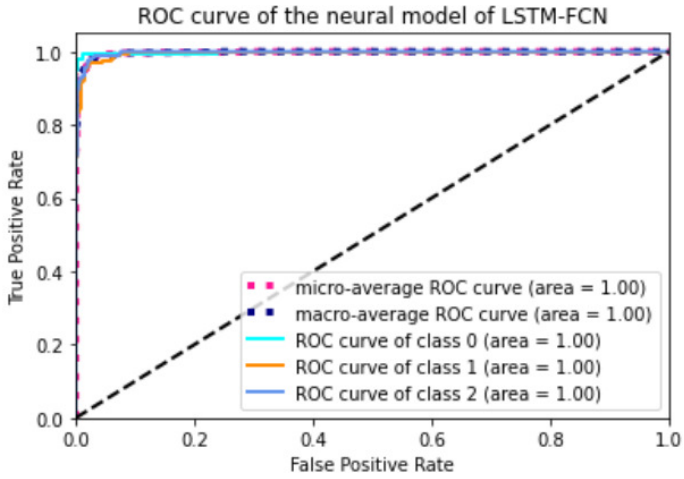


Figure A5. Classification performance of the LSTM-FCN neural classifier. Class 0: normal patient, class 1: patient with glucose intolerance, and class 2: patient with diabetes mellitus.

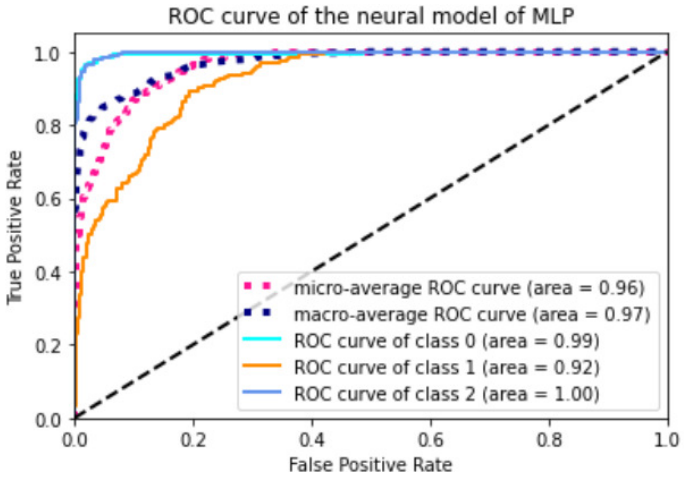


Figure A6. Classification performance of the MLP neural classifier. Class 0: normal patient, class 1: patient with glucose intolerance, and class 2: patient with diabetes mellitus.

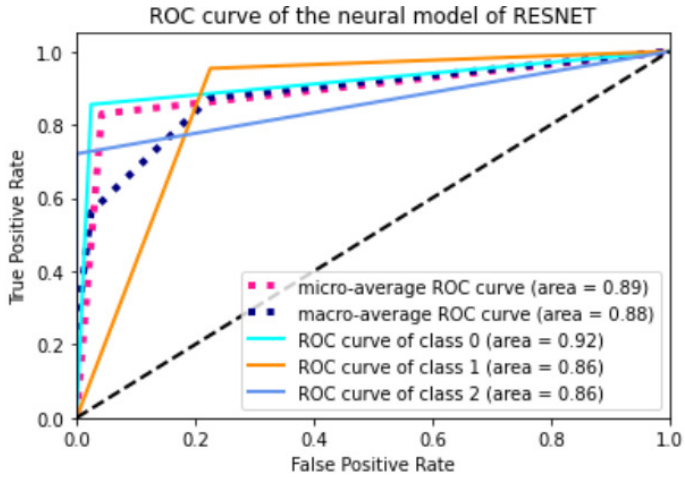


Figure A7. Classification performance of the RESNET neural classifier. Class 0: normal patient, class 1: patient with glucose intolerance, and class 2: patient with diabetes mellitus.

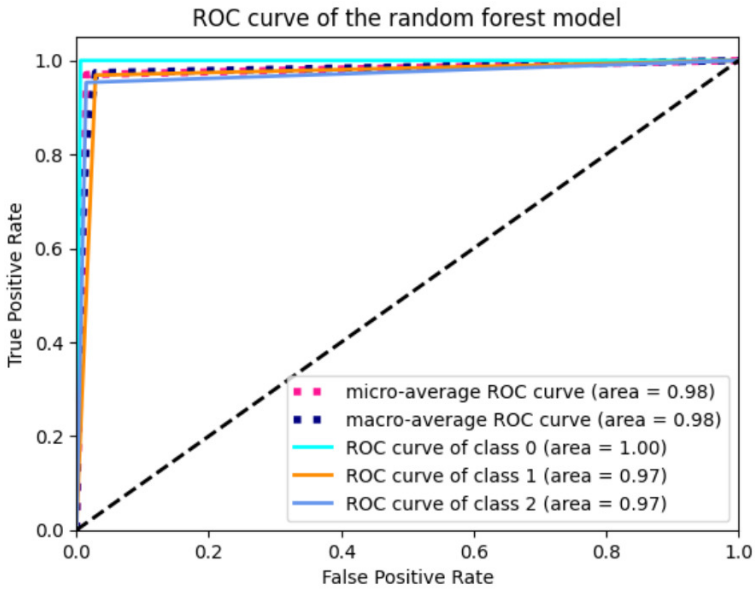


Figure A8. Classification performance of the random forest model. Class 0: normal patient, class 1: patient with glucose intolerance, and class 2: patient with diabetes mellitus.

References

1. Stuart, P.J.; Crooks, S.; Porton, M. An interventional program for diagnostic testing in the emergency department. *Med. J. Aust.* **2002**, *177*, 131–134. [CrossRef] [PubMed]
2. Pölsterl, S.; Conjeti, S.; Navab, N.; Katouzian, A. Survival analysis for high-dimensional, heterogeneous medical data: Exploring feature extraction as an alternative to feature selection. *Artif. Intell. Med.* **2016**, *72*, 1–11. [CrossRef] [PubMed]
3. Kumar, D.; Jain, N.; Khurana, A.; Mittal, S.; Satapathy, S.C.; Senkerik, R.; Hemanth, J.D. Automatic detection of white blood cancer from bone marrow microscopic images using convolutional neural networks. *IEEE Access* **2020**, *8*, 142521–142531. [CrossRef]
4. Javeed, A.; Zhou, S.; Yongjian, L.; Qasim, I.; Noor, A.; Nour, R. An intelligent learning system based on random search algorithm and optimized random forest model for improved heart disease detection. *IEEE Access* **2019**, *7*, 180235–180243. [CrossRef]
5. Kulkarni, N.N.; Bairagi, V.K. Extracting salient features for EEG-based diagnosis of Alzheimer's disease using support vector machine classifier. *IETE J. Res.* **2017**, *63*, 11–22. [CrossRef]
6. Kumari, V.A.; Chitra, R. Classification of diabetes disease using support vector machine. *Int. J. Eng. Res. Appl.* **2013**, *3*, 1797–1801.
7. Uchida, T.; Kanamori, T.; Teramoto, T.; Nonaka, Y.; Tanaka, H.; Nakamura, S.; Murayama, N. Identifying Glucose Metabolism Status in Nondiabetic Japanese Adults Using Machine Learning Model with Simple Questionnaire. *Comput. Math. Methods Med.* **2022**, *2022*, 1026121. [CrossRef] [PubMed]
8. Sejnowski, T.J.; Rosenberg, C.R. Parallel networks that learn to pronounce English text. *Complex Syst.* **1987**, *1*, 145–168.
9. Zaremba, W.; Sutskever, I.; Vinyals, O. Recurrent neural network regularization. *arXiv* **2014**, arXiv:1409.2329.
10. Verner, A.; Mukherjee, S. An LSTM-Based Method for Detection and Classification of Sensor Anomalies. In Proceedings of the 2020 5th International Conference on Machine Learning Technologies, Beijing, China, 19–21 June 2020; pp. 39–45.
11. Lee, X.Y.; Kumar, A.; Vidyaratne, L.; Rao, A.R.; Farahat, A.; Gupta, C. An ensemble of convolution-based methods for fault detection using vibration signals. *arXiv* **2023**, arXiv:2305.05532.
12. Oh, S.L.; Hagiwara, Y.; Raghavendra, U.; Yuvaraj, R.; Arunkumar, N.; Murugappan, M.; Acharya, U.R. A deep learning approach for Parkinson's disease diagnosis from EEG signals. *Neural Comput. Appl.* **2020**, *32*, 10927–10933. [CrossRef]
13. Maragatham, G.; Devi, S. LSTM model for prediction of heart failure in big data. *J. Med Syst.* **2019**, *43*, 111. [CrossRef] [PubMed]
14. Sheng, B.; Chen, X.; Li, T.; Ma, T.; Yang, Y.; Bi, L.; Zhang, X. An overview of artificial intelligence in diabetic retinopathy and other ocular diseases. *Front. Public Health* **2022**, *10*, 971943. [CrossRef] [PubMed]
15. Nomura, A.; Noguchi, M.; Kometani, M.; Furukawa, K.; Yoneda, T. Artificial intelligence in current diabetes management and prediction. *Curr. Diabetes Rep.* **2021**, *21*, 61. [CrossRef]
16. Contreras, I.; Vehi, J. Artificial intelligence for diabetes management and decision support: Literature review. *J. Med. Internet Res.* **2018**, *20*, e10775. [CrossRef] [PubMed]
17. Chaki, J.; Ganesh, S.T.; Cidham, S.; Theertan, S.A. Machine learning and artificial intelligence based Diabetes Mellitus detection and self-management: A systematic review. *J. King Saud. Univ.-Comput. Inf. Sci.* **2022**, *34*, 3204–3225. [CrossRef]
18. Association, A.D. Classification and diagnosis of diabetes: Standards of Medical Care in Diabetes—2020. *Diabetes Care* **2020**, *43*, S14–S31. [CrossRef] [PubMed]
19. Nathan, D.M.; Group, D.R. The diabetes control and complications trial/epidemiology of diabetes interventions and complications study at 30 years: Overview. *Diabetes Care* **2014**, *37*, 9–16. [CrossRef]
20. Punthakee, Z.; Goldenberg, R.; Katz, P. Definition, classification and diagnosis of diabetes, prediabetes and metabolic syndrome. *Can. J. Diabetes* **2018**, *42*, S10–S15. [CrossRef]
21. Association, A.D. Guide to Diagnosis and Classification of Diabetes Mellitus and Other Categories of Glucose Intolerance. *Diabetes Care* **1997**, *20*, S21. [CrossRef]
22. Bello-Chavolla, O.Y.; Rojas-Martinez, R.; Aguilar-Salinas, C.A.; Hernández-Avila, M. Epidemiology of diabetes mellitus in Mexico. *Nutr. Rev.* **2017**, *75*, 4–12. [CrossRef] [PubMed]
23. Martínez Basila, A.; Maldonado Hernández, J.; López Alarcón, M. Métodos diagnósticos de la resistencia a la insulina en la población pediátrica. *Boletín Méd. Hosp. Infant. México* **2011**, *68*, 397–404.
24. Jia, F.; Lei, Y.; Lin, J.; Zhou, X.; Lu, N. Deep neural networks: A promising tool for fault characteristic mining and intelligent diagnosis of rotating machinery with massive data. *Mech. Syst. Signal Process.* **2016**, *72*, 303–315. [CrossRef]
25. Ogunmolu, O.; Gu, X.; Jiang, S.; Gans, N. Nonlinear systems identification using deep dynamic neural networks. *arXiv* **2016**, arXiv:1610.01439.
26. Loh, H.W.; Ooi, C.P.; Palmer, E.; Barua, P.D.; Dogan, S.; Tuncer, T.; Baygin, M.; Acharya, U.R. GaborPDNet: Gabor transformation and deep neural network for Parkinson's disease detection using EEG signals. *Electronics* **2021**, *10*, 1740. [CrossRef]
27. Zhai, X.; Ali, A.A.S.; Amira, A.; Bensaali, F. MLP neural network based gas classification system on Zynq SoC. *IEEE Access* **2016**, *4*, 8138–8146. [CrossRef]
28. Lim, T.Y.; Ratnam, M.M.; Khalid, M.A. Automatic classification of weld defects using simulated data and an MLP neural network. *Insight-Non Test. Cond. Monit.* **2007**, *49*, 154–159. [CrossRef]
29. Girshick, R.; Donahue, J.; Darrell, T.; Malik, J. Rich feature hierarchies for accurate object detection and semantic segmentation. In Proceedings of the IEEE Conference on Computer Vision and Pattern Recognition, Columbus, OH, USA, 23–28 June 2014; pp. 580–587.

30. Zheng, Y.; Liu, Q.; Chen, E.; Ge, Y.; Zhao, J.L. Time series classification using multi-channels deep convolutional neural networks. In *Web-Age Information Management. WAIM 2014. Lecture Notes in Computer Science*; Li, F., Li, G., Hwang, S.W., Yao, B., Zhang, Z., Eds.; Springer: Cham, Switzerland, 2014; pp. 298–310.
31. Krizhevsky, A.; Sutskever, I.; Hinton, G.E. Imagenet classification with deep convolutional neural networks. *Adv. Neural Inf. Process. Syst.* **2012**, *25*, 1097–1105. [CrossRef]
32. Albawi, S.; Bayat, O.; Al-Azawi, S.; Ucan, O.N. Social touch gesture recognition using convolutional neural network. *Comput. Intell. Neurosci.* **2018**, *2018*, 1881. [CrossRef]
33. Hochreiter, S.; Schmidhuber, J. Long short-term memory. *Neural Comput.* **1997**, *9*, 1735–1780. [CrossRef]
34. Siami-Namini, S.; Tavakoli, N.; Namin, A.S. The performance of LSTM and BiLSTM in forecasting time series. In Proceedings of the 2019 IEEE International Conference on Big Data (Big Data), Los Angeles, CA, USA, 9–12 December 2019; pp. 3285–3292. [CrossRef]
35. Koley, B.; Dey, D. An ensemble system for automatic sleep stage classification using single channel EEG signal. *Comput. Biol. Med.* **2012**, *42*, 1186–1195. [CrossRef] [PubMed]
36. Karim, F.; Majumdar, S.; Darabi, H.; Chen, S. LSTM fully convolutional networks for time series classification. *IEEE Access* **2017**, *6*, 1662–1669. [CrossRef]
37. Kim, Y.; Sa, J.; Chung, Y.; Park, D.; Lee, S. Resource-efficient pet dog sound events classification using LSTM-FCN based on time-series data. *Sensors* **2018**, *18*, 4019. [CrossRef] [PubMed]
38. He, K.; Zhang, X.; Ren, S.; Sun, J. Deep residual learning for image recognition. In Proceedings of the IEEE Conference on Computer Vision and Pattern Recognition, Las Vegas, NV, USA, 27–30 June 2016; pp. 770–778.
39. Russakovsky, O.; Deng, J.; Su, H.; Krause, J.; Satheesh, S.; Ma, S.; Huang, Z.; Karpathy, A.; Khosla, A.; Bernstein, M.; et al. Imagenet large scale visual recognition challenge. *Int. J. Comput. Vis.* **2015**, *115*, 211–252. [CrossRef]
40. Lin, T.Y.; Maire, M.; Belongie, S.; Hays, J.; Perona, P.; Ramanan, D.; Dollár, P.; Zitnick, C.L. Microsoft coco: Common objects in context. In *Computer Vision – ECCV 2014. ECCV 2014. Lecture Notes in Computer Science*; Fleet, D., Pajdla, T., Schiele, B., Tuytelaars, T., Eds.; Springer: Cham, Switzerland, 2014; pp. 740–755.
41. Ferrandez, S.M.; Harbison, T.; Weber, T.; Sturges, R.; Rich, R. Optimization of a truck-drone in tandem delivery network using k-means and genetic algorithm. *J. Ind. Eng. Manag. (JIEM)* **2016**, *9*, 374–388. [CrossRef]
42. Shan, P. Image segmentation method based on K-mean algorithm. *EURASIP J. Image Video Process.* **2018**, *2018*, 68. [CrossRef]
43. Köbberling, J.; Berninger, D. Natural History of Glucose Tolerance in Relatives of Diabetic Patients: Low Prognostic Value of the Oral Glucose Tolerance Test. *Diabetes Care* **1980**, *3*, 21–26. [CrossRef] [PubMed]
44. Kuo, F.Y.; Cheng, K.C.; Li, Y.; Cheng, J.T. Oral glucose tolerance test in diabetes, the old method revisited. *World J. Diabetes* **2021**, *12*, 786. [CrossRef]
45. Pollak, F.; Araya, V.; Lanas, A.; Sapunar, J.; Arrese, M.; Aylwin, C.G.; Bezanilla, C.G.; Carrasco, E.; Carrasco, F.; Codner, E.; et al. II Consenso de la Sociedad Chilena de Endocrinología y Diabetes sobre resistencia a la insulina. *Rev. Méd. Chile* **2015**, *143*, 627–636. [CrossRef]
46. Bailes, B.K. Diabetes Mellitus and its Chronic Complications. *AORN J.* **2002**, *76*, 265–282. . [CrossRef]
47. Dalla Man, C.; Rizza, R.A.; Cobelli, C. Meal simulation model of the glucose-insulin system. *IEEE Trans. Biomed. Eng.* **2007**, *54*, 1740–1749. [CrossRef] [PubMed]
48. Man, C.D.; Micheletto, F.; Lv, D.; Breton, M.; Kovatchev, B.; Cobelli, C. The UVA/PADOVA type 1 diabetes simulator: New features. *J. Diabetes Sci. Technol.* **2014**, *8*, 26–34. [CrossRef] [PubMed]
49. Visentin, R.; Dalla Man, C.; Cobelli, C. One-day Bayesian cloning of type 1 diabetes subjects: Toward a single-day UVA/Padova type 1 diabetes simulator. *IEEE Trans. Biomed. Eng.* **2016**, *63*, 2416–2424. [CrossRef] [PubMed]
50. Sánchez, O.D.; Ruiz-Velázquez, E.; Alanís, A.Y.; Quiroz, G.; Torres-Treviño, L. Parameter estimation of a meal glucose–insulin model for TIDM patients from therapy historical data. *IET Syst. Biol.* **2019**, *13*, 8–15. [CrossRef] [PubMed]
51. Group, N.D.D. Classification and diagnosis of diabetes mellitus and other categories of glucose intolerance. *Diabetes* **1979**, *28*, 1039–1057.
52. Kuschinski, N.; Christen, J.A.; Monroy, A.; Alavez, S. Modeling oral glucose tolerance test (ogtt) data and its bayesian inverse problem. *arXiv* **2016**, arXiv:1601.04753.
53. Cerda, J.; Cifuentes, L. Uso de curvas ROC en investigación clínica: Aspectos teórico-prácticos. *Rev. Chil. Infectología* **2012**, *29*, 138–141. [CrossRef]

Disclaimer/Publisher's Note: The statements, opinions and data contained in all publications are solely those of the individual author(s) and contributor(s) and not of MDPI and/or the editor(s). MDPI and/or the editor(s) disclaim responsibility for any injury to people or property resulting from any ideas, methods, instructions or products referred to in the content.